# Surface Molecular Aggregation Structure and Surface Molecular Motions of High-Molecular-Weight Polystyrene/Low-Molecular-Weight Poly(methyl methacrylate) Blend Films

**Keiji Tanaka, Atsushi Takahara, and Tisato Kajiyama***

*Department of Materials Physics & Chemistry, Graduate School of Engineering, Kyushu University, 6-10-1 Hakozaki, Higashi-ku, Fukuoka 812-81, Japan*

*Received July 7, 1997; Revised Manuscript Received October 22, 1997*

ABSTRACT: Surface molecular aggregation structure and surface molecular motions of high-molecular-weight polystyrene/low-molecular-weight poly(methyl methacrylate) (HMW-PS/LMW-PMMA) blend films were investigated on the basis of X-ray photoelectron spectroscopic measurements and scanning force microscopic observations. Monodisperse PS with $M_n$ = 1450k, where $M_n$ denotes the number-average molecular-weight, and monodisperse PMMAs with $M_n$ 1.2k, 4.2k, 40.5k, 144k, and 387k were used as HMW-PS and LMW-PMMAs, respectively. Static contact angle measurements revealed that the magnitudes of surface free energy, $\gamma$, of PMMAs for all $M_n$s studied here were higher than that of PS with $M_n$ = 1450K. In the case of the (HMW-PS/LMW-PMMA) blend films, in which the $M_n$ for each PMMA was less than 144K, PMMA was preferentially segregated at the air−polymer interface, even though PMMA had a main chain with a higher $\gamma$ compared with that of PS. It was found from scanning viscoelasticity microscopic measurements that the surface molecular motion of the (PS with $M_n$ = 1450k/PMMA with $M_n$ = 4.2k) blend film was fairly activated in comparison with that of the bulk one due to the surface segregation of LMW-PMMA. The surface enrichment of LMW-PMMA can be explained by enthalpic and entropic terms as follows. (1) Since the magnitudes of $\gamma$ of both chain end groups of a polymer chain synthesized by an ordinary living anionic polymerization are smaller than that of the main chain part, the chain end groups are preferentially segregated at the surface. Therefore, the chain end effect at the air−polymer interface becomes more remarkable with a decrease of $M_n$, due to an increases in the number density of chain end groups. (2) Since polymeric chains existing in a surface region are compressed along the direction perpendicular to the film surface, the surface chains take smaller conformational entropy in a confined state compared with that of bulk chains. The difference in conformational entropy between the surface chain and the bulk one, that is, the conformational entropic penalty of the polymeric chain at the surface, decreases with a decrease in $M_n$. Then, when the enthalpic and entropic effects mentioned above overcome the $\gamma$ difference of main chain parts between PS and PMMA, PMMA with higher $\gamma$ is stably enriched at the blend film surface.

## Introduction

When polymers are used as functional materials, the surface characteristics play an important role and determine the functional performance.[1] In order to design the polymer surface with characteristic functionalities, it is necessary to control surface aggregation structure and surface orientation of polymeric chains as well as surface molecular motions. Molecular aggregation structure and molecular motions at the air−polymer interface are quite different from those in the bulk region due to the difference of free energy state between surface and bulk.[2]

The surface chemical composition of polymer blends has been extensively investigated in the past decade, both experimentally[3−6] and theoritically.[7−9] Most studies revealed that the lower surface free energy $\gamma$ component was enriched at the air−polymer interface in order to minimize the magnitude of interfacial free energy. For instance, in the case of the miscible polystyrene/poly(vinyl methyl ether) (PS/PVME) blend film, X-ray photoelectron spectroscopic (XPS) and surface tension measurements revealed that the surface was covered with PVME chains with lower $\gamma$.[5,6] Also, in the case of the (PS/deuterated PS) blend film, it was revealed from dynamic secondary ion mass spectroscopic (DSIMS) and forward recoil elastic scattering (FRES) measurements that deuterated PS was preferentially segregated at the film surface, since the magnitude of $\gamma$ for deuterated PS is lower than that of PS due to the lower polarizability of the C−D bond compared with that of the C−H one.[10]

It is generally accepted that the effect of chain end groups on the surface structure and the surface molecular motions cannot be ignored, especially in the case of the polymeric materials with smaller $M_n$, where $M_n$ denotes the number-average molecular-weight.[11−13] If the magnitude of $\gamma$ for the chain end groups, $\gamma_e$, is lower than that of the main chain part, $\gamma_m$, then the chain end groups are preferentially localized at the surface,[14−15] whereas, in the case of $\gamma_e > \gamma_m$, the chain end groups migrate deeply into the surface interior region.[16] Monodisperse polymers prepared by an anionic polymerization using butyllithium as an initiator have two chain ends composed of the initiator fragment and the repeating units, terminated with a proton. The magnitude of $\gamma$ for a *sec*-butyl end group is ca. 30.0 mJ·m$^{-2}$ and is generally smaller than $\gamma_m$ for vinyl polymers.[17] Also, the magnitude of $\gamma$ for the repeating units terminated with a proton might be lower than $\gamma_m$, because the magnitude of $\gamma$ is proportional to the density.[18] Therefore, since both chain end groups of monodisperse polymer synthesized by using butyllithium as an initia-

* To whom correspondence should be addressed. Tel.: +81-92-642-3558. Fax: +81-92-651-5606. E-mail: tkajitcf@mbox.nc.kyushu-u.ac.jp.

S0024-9297(97)00986-8 CCC: $15.00 
Published on Web 01/17/1998

tor have a lower magnitude of $\gamma$ compared with that of the main chain part, it seems reasonable that both chain end groups might be localized at the surface. Since the chain end group concentration is reciprocally proportional to $M_n$, the effect of $M_n$ on the surface structure and surface molecular motions for the polymer blend films with low $M_n$ becomes fairly important. In the following, especially in the case of the $\gamma$ term without the subscript "e" or "m", $\gamma$ means the surface free energy obtained from the experiment.

Wattenbarger et al. pointed out that a polymer chain was compressed at the film surface on the basis of computer calculation under the assumption of a two-dimensional lattice.[19] Since a polymer chain at the surface might be compressed along the direction perpendicular to the film surface, a restricted polymer chain has a smaller conformational entropy compared with that of a polymer chain in the bulk region. The difference in conformational entropy of polymer chains at the surface and in the bulk, that is, the conformational entropy loss of a polymeric chain at the surface, depends somewhat on the magnitude of $M_n$. Thus, the surface might be favorably covered by the lower $M_n$ component because a longer polymer chain at the surface suffers a severe conformational entropic penalty.[20] Kumar et al. investigated the surface segregation of the binary polymer mixture with different $M_n$s and the same $\gamma$, such as the polymer mixture with bimodal $M_n$ distribution based on a mean-field lattice model, and revealed that the lower $M_n$ component was preferentially segregated at the film surface due to a purely entropic effect.[21]

Thus, it should be quite interesting to study the case in which the components segregate at the film surface, when the effect of $M_n$ on the surface segregation of polymeric chains conflicts with the effect of $\gamma_m$, that is, the lower $M_n$ component has a higher magnitude $\gamma_m$. The purpose of this study is to investigate the surface aggregation structure and the surface molecular motions of the high-molecular-weight PS/low-molecular-weight poly(methyl methacrylate) (HMW-PS/LMW-PMMA) blend film, in which PMMA has a shorter main chain length but a higher $\gamma_m$ compared with those of PS. In the case of the ordinary (PS/PMMA) blend, that is, the $M_n$ of PS is comparable to that of PMMA, it has been revealed from XPS measurements and scanning force microscopic (SFM) observations that the PS component is enriched at the film surface.[22] In this case, the surface segregation of PS can be explained in terms of only the discrepancy of $\gamma_m$ between PS and PMMA.

## Experimental Section

**Materials.** Polymers used in this study were monodisperse PS and PMMA. PS with $M_n$ = 1450k and polydispersity, $M_w/M_n$, of 1.06, where $M_w$ denotes the weight-average molecular-weight, was purchased from Polymer Laboratories Co., Ltd. The bulk glass transition temperature, $T_g$, of PS evaluated by differential scanning calorimetry (DSC) was 380.7 K. PMMAs with various $M_n$ were synthesized in tetrahydrofuran by a living anionic polymerization at 196 K using *sec*-butyllithium-added 1,1-diphenylethylene as an initiator. The products were purified by fractional precipitation. Table 1 shows the magnitudes of $M_n$ and $M_w/M_n$ of PMMAs determined via gel permeation chromatography with polystyrene standards. Also, Table 1 shows the bulk $T_g$s of monodisperse PMMAs measured by DSC.

**Blend Film Preparation.** A (HMW-PS/LMW-PMMA) blend solution was prepared by mixing individual toluene solutions of PS and PMMA. The $M_n$ of PS was fixed on 1450K, whereas, that of PMMA was changed from 1.2k to 387k. The blend ratio was designated as (weight %/weight %). The (HMW-PS/LMW-PMMA) blend films were coated onto a cleaned silicon wafer with native oxide layer from a toluene solution by a spin coating at 2 krpm. The blend film was dried under vacuum for 72 h at room temperature. The thickness of the (HMW-PS/LMW-PMMA) blend film evaluated from ellipsometric measurement ranged from 600 nm to 700 nm.

**Table 1. Characterizations of PS and PMMA Used in This Study**

| | $M_n$ | $M_w/M_n$ | $T_g$ (K) |
|---|---|---|---|
| PS | 1450k | 1.04 | 380.7 |
| PMMA | 1.2k | 1.22 | 366.4 |
| | 4.2k | 1.10 | 375.3 |
| | 40.5k | 1.05 | 398.3 |
| | 144k | 1.05 | 399.3 |
| | 387k | 1.13 | 398.6 |

**Surface Characterizations.** The surface chemical composition of the (HMW-PS/LMW-PMMA) blend film was investigated on the basis of X-ray photoelectron spectroscopic (XPS) measurement. The XPS spectra were obtained with ESCA 850 X-ray photoelectron spectrometer (Shimadzu Co. Ltd.). The XPS measurement was performed with MgK$\alpha$ X-ray source at 8 kV and 30 mA. The main chamber of XPS was maintained at $\sim 10^{-6}$ Pa. All $C_{1s}$ peaks corresponding to the neutral carbon were assigned a binding energy of 285.0 eV to correct for the charging energy shift. The analytical depth of XPS, $d$ from the outermost surface is defined by

$$d = 3\lambda \sin\theta \qquad (1)$$

where $\lambda$ and $\theta$ are the inelastic mean-free path of photoelectron in the solids and the emission angle of photoelectron, respectively.[23] Since the magnitude of $\theta$ was 30° in this study, the magnitude of $d$ evaluated by eq 1 was ca. 5.4 nm.

The surface morphology of the (HMW-PS/LMW-PMMA) blend film was observed by using atomic force microscopy (AFM). The AFM image was obtained by using an SPA 300 with an SPI 3700 controller (Seiko Instruments Industry Co., Ltd.) at 293 K in air. The cantilever (Olympus Co., Ltd.) used for AFM observation was microfabricated from $Si_3N_4$, and its spring constant was 0.022 N·m$^{-1}$.

In order to evaluate the surface molecular motion of the (HMW-PS/LMW-PMMA) blend film, surface viscoelasticity measurements[24] were performed by using an SFM at 293 K in air under a repulsive force region. The modulation frequency and the modulation amplitude were 4 kHz and 1.0 nm, respectively. The cantilever used for surface viscoelastic measurement by SFM was microfabricated from $Si_3N_4$, and its spring constant was 0.09 N·m$^{-1}$.

## Results and Discussion

**Surface Free Energy.** In the case of $\gamma_e < \gamma_m$, it is reasonable to consider that the magnitude of $\gamma$ for polymeric solids decreases with a decrease in $M_n$ because the concentration of chain end groups increases with a decrease in $M_n$.[25] Since $\gamma$ is one of the factors that controls the surface characteristics, it is necessary to evaluate the $M_n$ dependence of its magnitude. The magnitude of $\gamma$ for the monodisperse PMMA film was evaluated by static contact angle measurements with water and methylene iodide as probe liquids on the basis of the Owens's procedure.[26] Figure 1 shows the $M_n$ dependence of $\gamma$ for the PMMA films. The broken line in Figure 1 denotes the magnitude of $\gamma$ for the monodisperse PS film with $M_n$ = 1450k, and its magnitude was 40.9 mJ·m$^{-2}$. In the cases of the PMMA films with $M_n$s of 40.5k, 144k, and 387k, the magnitudes of $\gamma$ were almost 44.3 mJ·m$^{-2}$, and no distinct $M_n$ dependence of $\gamma$ was observed. On the other hand, the magnitude of

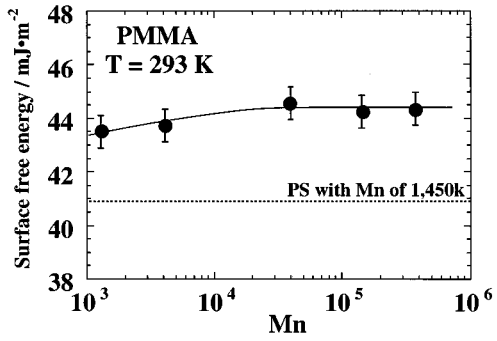


**Figure 1.** Molecular weight dependence of surface free energy, $\gamma$, for PMMA. Dashed horizontal line shows the magnitude of $\gamma$ for PS with $M_n$ = 1450k. The magnitude of $\gamma$ was evaluated by using water and methylene iodine as a probe liquid on the basis of Owens's procedure.

$\gamma$ slightly decreased with $M_n$ for the PMMA films with $M_n$ < 4.2K, and the magnitudes of $\gamma$ for $M_n$s = 1.2K and 4.2K were 43.5 and 43.7 mJ·m$^{-2}$, respectively. These results indicate that the PMMAs used here are the higher $\gamma$ component in comparison with PS, with $M_n$ = 1450K.

**Surface Composition.** In order to investigate the surface chemical composition of (HMW-PS/LMW-PMMA) blend films, XPS measurement was carried out. Figure 2 shows the XPS C1s spectra of the as-cast (HMW-PS/LMW-PMMA) film and, also, the HMW-PS and the LMW-PMMA homopolymer films at a photoelectron emission angle of 30°. The $C_{1s}$ peaks corresponding to neutral, ether, and carbonyl carbons were observed at 285.0, 286.5, and 289.0 eV, respectively. Also, the $C_{1s}$ shake-up peak corresponding to the $\pi-\pi^*$ transition of the benzene ring was observed at 291.5−292.0 eV. Curve-fitting of the $C_{1s}$ spectra was achieved on the basis of a nonlinear least-squares method. A Gaussian function was assumed for each curve. Then, the $C_{1s}$ spectra were separated into the four peaks corresponding to neutral, ether, and carbonyl carbons and the shake-up of the $\pi-\pi^*$ transition of the aromatic group. The surface PMMA weight fraction, $\omega$, was calculated by using eq 2, where $I_i$ is the integrated

$$\frac{I_{C=O} + I_{C-O}}{I_{total}} = \frac{2\omega/M_{MMA}}{8(1-\omega)/M_S + 5\omega/M_{MMA}} \qquad (2)$$

intensity of a core electron photoemission spectrum, and $M_S$ and $M_{MMA}$ are the molecular-weights for styrene and methyl methacrylate monomer units, respectively.

Figure 3 shows the blend ratio dependence of the surface PMMA weight fraction for the (HMW-PS/LMW-PMMA) blend films as functions of annealing temperature and $M_n$ for PMMA. The symbols ●, ○, and ■ show the surface PMMA fractions for the as-cast (HMW-PS/LMW-PMMA) blend film and those annealed at 353 and 393 K for 24 h, respectively. The dashed line denotes the surface composition corresponding to the blend ratio, that is, the bulk composition. It is apparently a general tendency from Figure 3 that the PMMA fraction of the (HMW-PS/LMW-PMMA) blend film surface increased with the blend ratio of PMMA. In the case of $M_n$ of PMMA from 1.2k to 40.5k, the surface PMMA weight fraction was much higher than the blend ratio of PMMA. Then, it seems reasonable to conclude that PMMA is preferentially segregated at the blend film surface, even though the PMMA component has a higher $\gamma$ compared with that of PS. Surprisingly, the

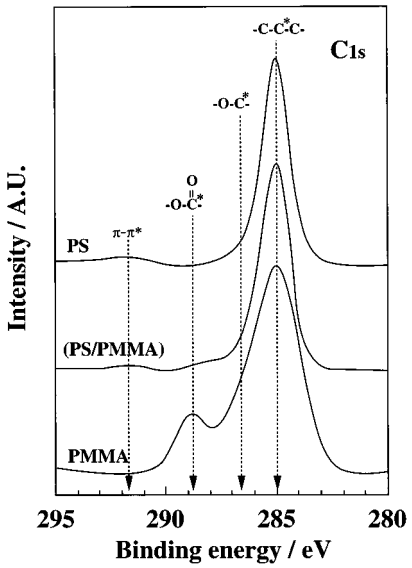


**Figure 2.** XPS $C_{1s}$ core-level spectra of typical as-cast (HMW-PS/LMW-PMMA) blend film and PS and PMMA homopolymer films.

surface PMMA fractions for the as-cast and the annealed (PS1450k/PMMA1.2k) (99.5/0.5 w/w) films were 17.1% and 19.0%, respectively; in other words, the surface PMMA fraction was ca. 36−38 times as much as the bulk blend ratio of PMMA. In this case, no apparent annealing effect on the surface composition was observed, as shown in Figure 3a. Although the surface PMMA fraction slightly increased after annealing for the (PS1450k/PMMA4.2k) blend film, no distinct annealing temperature effect on the surface composition was observed, as shown in Figure 3b. In the case of the (PS1450k/PMMA40.5k) blend film, the surface enrichment of the LMW-PMMA was observed as shown in Figure 3c in a similar fashion to the (PS1450k/PMMA1.2k) and (PS1450k/PMMA4.2k) blend films. However, when the surface composition was compared among the (PS1450k/PMMA1.2k), (PS1450k/PMMA4.2k), (PS1450k/PMMA40.5k), and (PS1450k/PMMA144k) blend films with the same bulk composition, it was clear that the magnitude of the surface PMMA fraction decreased with an increase in $M_n$ of PMMA. This result indicates that the surface segregation of a certain component for the binary polymer blend film is determined by the conflict between the $\gamma_m$ difference and the $M_n$ one for the PS and PMMA components. Moreover, when the $M_n$ of PMMA increased to 387k, the surface PMMA weight fraction became lower than the blend ratio of PMMA, as shown in Figure 3e. That is, the PMMA component was not enriched at the blend film surface, since the $\gamma_m$ effect on the surface segregation becomes more dominant than the $M_n$ effect. The surface molecular aggregation structure for the (PS1450k/PMMA387k) film can be explained mainly in terms of the $\gamma_m$ difference between PS and PMMA.

In the case that polymeric chains at the blend film surface are frozen in a nonequilibrium state, for instance, due to fast evaporation of solvent during the film preparation process, the surface structure might start to reorganize into a quasi-equilibrium state upon annealing at a temperature above its surface $T_g$. In general, the degree of an increase in the surface PMMA fraction upon annealing increases with an increase in $M_n$, as shown in Figure 3a−c. This may indicate that

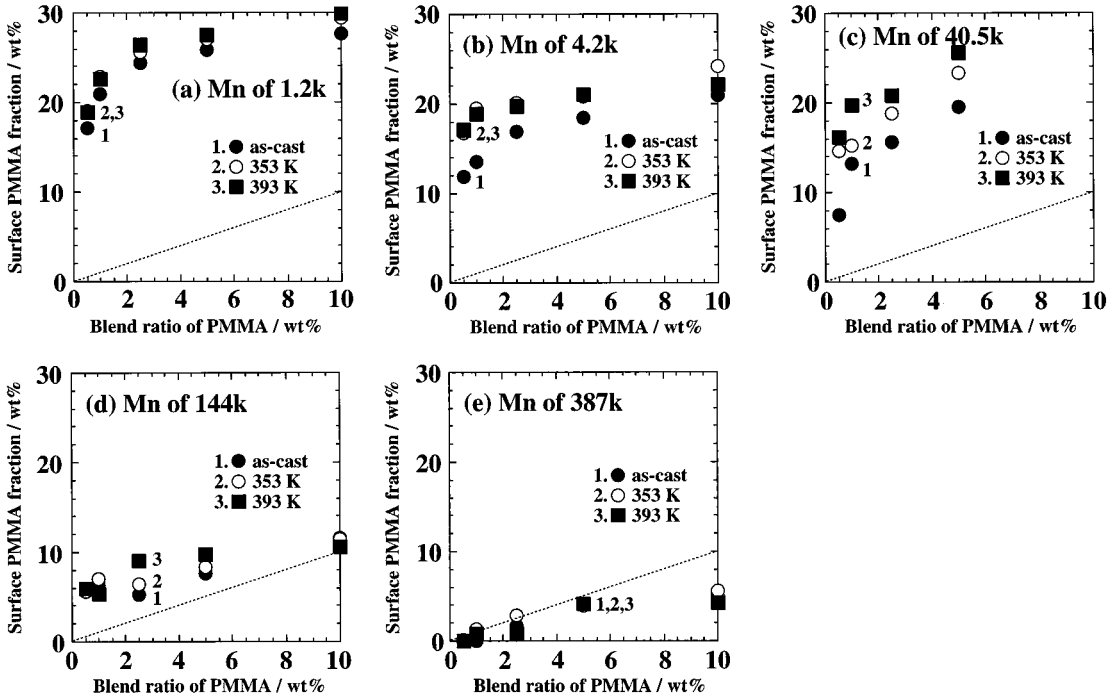


**Figure 3.** Blend ratio dependence of surface composition for the (PS1450k/LMW-PMMA) film as a function of annealing temperature. Each figure shows the relationship between surface composition and blend ratio for the (PS1450k/LMW-PMMA) with different $M_n$ values of PMMA. The filled circles denote the data of as-cast blend film. The open circles and the filled squares denote the data for the blend films annealed at 353 and 393 K, respectively.

the surfaces of these blend films are in a glass−rubber transition state, even at room temperature, especially in the case of PMMA with smaller $M_n$; moreover, the surface $T_g$ increases gradually with an increase in $M_n$. Therefore, it is reasonable to conclude that an annealing effect on the surface reorganization becomes more remarkable with an increase in $M_n$. The surface molecular motion of the (PS1450k/PMMA4.2k) blend film will be discussed in detail on the basis of surface viscoelastic measurement by SFM measurement in a later section.

**Surface Morphology and Surface Phase State.** In order to investigate the surface morphology and the surface phase state of the (HMW-PS/LMW-PMMA) blend film, SFM observations were carried out at 293 K in air. The bulk (PS/PMMA) blend system has an upper critical solution temperature (UCST)-type phase diagram.[27] Figure 4 shows the AFM image of the as-cast (PS1450k/PMMA4.2k) (99.0/1.0 w/w) blend film. No distinct domain structure was observed at the film surface, as shown in the AFM image. Also, no distinct contrast was observed on the basis of the surface viscoelastic measurement by SFM and lateral force microscopic (LFM) observations, which could evaluate surface mechanical properties and then distinguish different phases at the film surface.[13] Thus, it seems reasonable to conclude that the surface of the as-cast (PS1450k/PMMA4.2k) (99.0/1.0 w/w) blend film is in a homogeneous state, that is, a phase-mixing state. Also, the change of surface morphology such as phase-separated structure was not observed after annealing at 353 and 393 K for 24 h. Figure 5 shows the surface morphology of the as-cast (PS1450k/PMMA40.5k) (90.0/10.0 w/w) blend film. The well-defined island-like phase-separated structure with domains ca. 1 $\mu$m in diameter was observed at the film surface. Although the height of the domains was almost same as that of the matrix, the interfacial zone protruded from the film

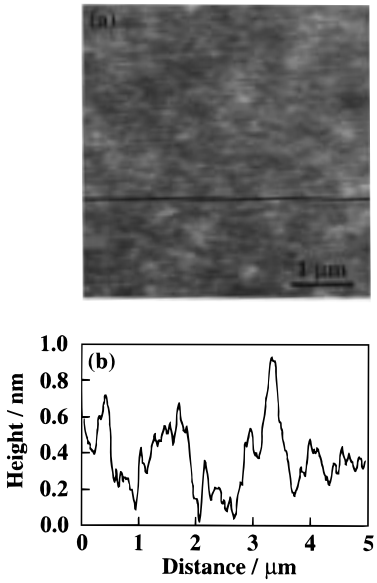


**Figure 4.** (a) AFM image and (b) sectional view along the line in the AFM image for the (PS1450k/PMMA4.2k) (99.0/1.0 w/w) blend film.

surface due to large repulsion between PS and PMMA segments, as shown in Figure 5b. Since the domain size increased with the blend ratio of PMMA, it seems reasonable to conclude that the domains are composed of the PMMA-rich phase. The surface area fraction of the PMMA-rich phase was much higher than the blend ratio of PMMA of 10.0%. This result clearly indicates that PMMA is enriched at the film surface, corresponding well with the XPS results. Figure 6 shows the AFM image of the (PS1450k/PMMA40.5k) (90.0/10.0 w/w) blend film after the surface etching treatment with acetonitrile for 15 min, which is a good solvent only for PMMA. Also, Figure 6b shows the sectional view along the line shown in the AFM image. Since the domains

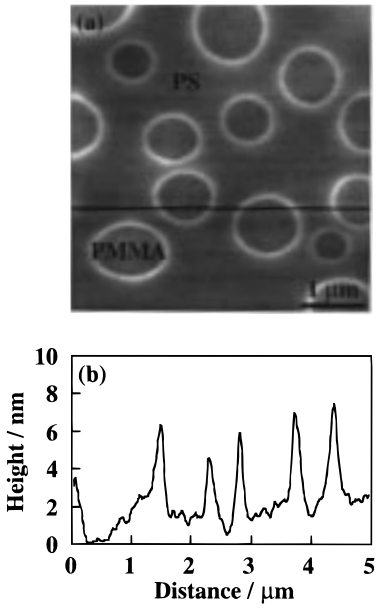


**Figure 5.** (a) AFM image and (b) sectional view along the line in the AFM image for the (PS1450k/PMMA40.5k) (90.0/10.0 w/w) blend film.

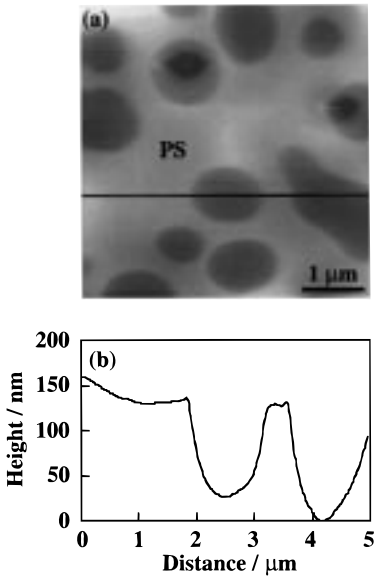


**Figure 6.** (a) AFM image and (b) sectional view along the line in the AFM image for the (PS1450k/PMMA40.5k) (90.0/10.0 w/w) blend film after the surface etching treatment with acetonitrile for 15 min.

are preferentially etched by surface treatment with acetonitrile, this result indicates again that the domains and the matrix regions are composed of the PMMA- and the PS-rich phases, respectively.

Table 2 summarizes the surface phase states of the (HMW-PS/LMW-PMMA) films determined by SFM observations. *H* and *S* denote the homogeneous state and the phase-separated one, respectively. Also, the *I* indicates an intermediate state, upon which the phase state depends. In general, since the interaction parameter between PS and PMMA segments is a large positive value, the homogeneous region on the phase diagram is fairly narrow with respect to the blend ratio.[27] However, in the case of the (PS1450k/PMMA1.2k) and (PS1450k/PMMA4.2k) blend films, the film surface was in a phase-mixing state for all blend ratios used here due to a large mixing entropy, $\Delta S_{mix}$, which is proportional to the reciprocal of the degree of polymerization, *N*, for the components:

$$\frac{\Delta S_{mix}}{n\,k_B} = -\left[\frac{\omega}{N_{PMMA}}\ln\omega + \frac{(1-\omega)}{N_{PS}}\ln(1-\omega)\right] \quad (3)$$

where $n$, $k_B$, and $\omega$ are total segment number, Boltzmann constant, and surface PMMA fraction, respectively. In the case of the (PS1450K/LMW-PMMA) blend film composed of PMMA with $M_n > 40.5$k, the surface was homogeneous if the blend ratio of PMMA was less than 0.5 wt %, as shown in Table 2.

**Table 2. Surface Phase State of Asymmetric (PS/PMMA) Blend Film**

| | PMMA fraction in bulk (wt %) | | | | |
|---|---|---|---|---|---|
| $M_n$ of PMMA | 0.5 | 1.0 | 2.5 | 5.0 | 10.0 |
| 1.2k | H | H | H | H | H |
| 4.2k | H | H | H | H | H |
| 40.5k | H | I | I | S | S |
| 144k | H | I | S | S | S |
| 387k | H | I | S | S | S |

[a] H, homogeneous; I, intermediate state; S, phase-separated states.

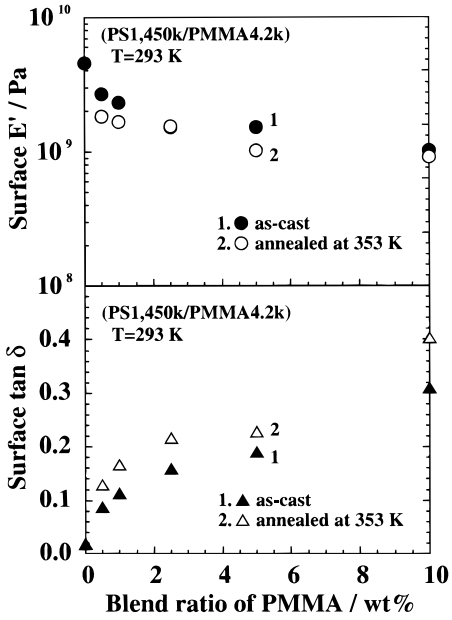


**Figure 7.** Blend ratio dependence of surface viscoelastic functions, surface $E'$, and surface tan $\delta$ for the (PS1450k/PMMA4.2k) blend film as a function of annealing temperature. The filled and the open symbols denote the data for the as-cast blend film and the one annealed at 353 K for 24 h, respectively.

**Surface Molecular Motion.** The surface viscoelastic measurement was carried out by SFM at 293 K in air in order to investigate surface molecular motion of the (HMW-PS/LMW-PMMA) blend film. Since the analysis of the surface molecular motion for the phase-separated blend film was quite complicated, the (PS1450k/PMMA4.2k) blend film, of which the surface was in a homogeneous state, was applied for surface viscoelastic measurement by SFM. The evaluation method for surface viscoelastic functions was published elsewhere.[13] Figure 7 shows the blend ratio dependence of surface dynamic storage modulus, $E'$, and surface loss tangent, tan $\delta$, for the (PS1450k/PMMA4.2k) blend film at 293 K. In the case of the PS film with $M_n = 1450$k,

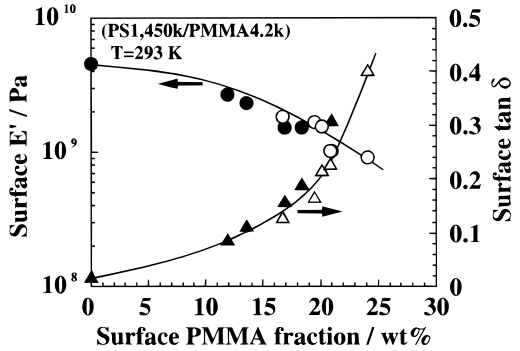


**Figure 8.** Surface composition dependence of surface $E'$ (circles) and surface tan $\delta$ (triangles) for the (PS1450k/PMMA4.2k) blend film. The filled and the open symbols denote the data for the as-cast blend film and the one annealed at 353 K for 24 h, respectively.

the magnitudes of surface $E'$ and surface tan $\delta$ were 4.6 GPa and 0.02, corresponding to those for a glassy state, respectively. The magnitudes of surface $E'$ and surface tan $\delta$ for the (PS1450k/PMMA4.2k) blend films gradually decreased and increased with an increase in the PMMA blend ratio, respectively; that is, the surface molecular motion became more vigorous with an increase in the blend ratio of PMMA. Also, the magnitudes of surface $E'$ and surface tan $\delta$ for the (PS1450k/PMMA4.2k) blend film decreased and increased with annealing at 353 K for 24 h, respectively, in comparison with those for the as-cast one. When the blend ratio of PMMA was increased and annealing was carried out at 353 K, the surface PMMA fraction increased. Then, it seems reasonable to investigate the surface viscoelastic functions as a function of the surface PMMA fraction. Figure 8 shows the surface PMMA fraction dependence of surface $E'$ and surface tan $\delta$ for the (PS1450k/PMMA4.2k) blend film. The filled and the open symbols denote the data for the as-cast blend film and the annealed one, respectively, at 353 K for 24 h. Figure 8 apparently shows that the surface composition dependence of surface $E'$ and surface tan $\delta$ can be plotted on each single master curve, respectively, and the activity of the surface molecular motion for the (PS1450k/PMMA4.2k) film is directly related to the PMMA fraction existing at the blend film surface. Therefore, this result clearly indicates that the surface of the (PS1450k/PMMA4.2k) blend films gradually approaches a glass−rubber transition state with an increase in the surface PMMA fraction even at 293 K, because it is generally accepted that the onset on the $E'$−temperature curve for the $\alpha_a$ dispersion and that on the tan $\delta$−temperature curve for the $\alpha_a$ absorption correspond well to $T_g$.[13] When LMW-PMMA is enriched at the air−polymer interface, the surface concentration of chain end groups increases in the case of $\gamma_e < \gamma_m$, because LMW-PMMA has a higher number density of chain end groups than PS with $M_n = 1450$K. The surface localization of chain end groups induces an excess free volume fraction at the film surface compared with the bulk phase.[13] Thus, it seems reasonable to conclude that the surface molecular motion of the (PS1450k/PMMA4.2k) becomes more vigorous with an increase in the surface PMMA fraction.

**Surface Segregation of LMW-PMMA.** In the case of the (PS1450k/LMW-PMMA) film composed of PMMAs with $M_n < 144$k, LMW-PMMA was preferentially segregated at the air−polymer interface, as shown in Figure 3a−c. The surface segregation of LMW-PMMA with larger $\gamma_m$ can be qualitatively explained mainly in terms of two factors, such as the enthalpic term based on the surface localization of chain end groups and the entropic term corresponding to the small conformational entropy loss and/or large translational entropy of LMW-PMMA chains existing at the surface. Yethiraj et al. investigated the surface segregation of the polymer blends on the basis of the chain stiffness and revealed that a stiffer chain is preferentially segregated at the surface.[28] However, since the statistical segment lengths of PS and PMMA are 0.68 and 0.69 nm, respectively,[29] it can be assumed here that the chain stiffness of PS is comparable to that of PMMA.

The total surface free energy, $\gamma_{total}$, at the (HMW-PS/LMW-PMMA) film surface has been discussed, taking account of the surface localization of chain end groups. The surface concentration of the chain end group, $C_{end}$, is written as follows:[11]

$$C_{end} = \frac{2}{N}\frac{R}{z} = \frac{2}{N^{1/2}}\frac{b}{z} \tag{4}$$

where $R$, $z$, and $b$ are end-to-end distance, depth from top surface, and statistical segment length, respectively. Thus, $\gamma_{total}$ can be expressed as follows:

$$\gamma_{total} = \omega\left[\gamma_{PMMA}\left(\left(1 - \frac{2}{N_{PMMA}^{1/2}}\frac{b_{PMMA}}{z}\right)/A\right) + \gamma_{PMMA-end}\left(\left(\frac{2}{N_{PMMA}^{1/2}}\frac{b_{PMMA}}{z}\right)/A\right)\right] + (1-\omega)\left[\gamma_{PS}\left(\left(1 - \frac{2}{N_{PS}^{1/2}}\frac{b_{PS}}{z}\right)A\right) + \gamma_{PS-end}\left(\left(\frac{2}{N_{PS}^{1/2}}\frac{b_{PS}}{z}\right)A\right)\right] \tag{5}$$

where $A$ represents unit area. For instance, in the case of the (PS1450k/PMMA4.2k) blend, when the magnitude of $\gamma_{end}$ is 30.0 mJ·m$^{-2}$ and $z = b$, the magnitude of $\gamma_{total}$ decreases with an increase in the surface PMMA fraction. Thus, it appears that the surface segregation of LMW-PMMA with higher $\gamma_m$ is preferable in the case of PMMA with small $M_n$.

The entropic effect on the surface segregation of the lower $M_n$ component has been discussed. Since an amorphous polymer chain in the bulk takes random coil conformation, its conformational entropy increases with an increase in $M_n$. On the other hand, polymeric chains existing at the film surface are compressed along the direction perpendicular to the film surface.[19] Thus, the conformational entropy of a chain at the film surface is fairly smaller than that in the bulk. The difference of conformational entropy between a polymeric chain existing at the surface and in the bulk, that is, the conformational entropic penalty of a chain at the surface, decreases with a decrease in $M_n$. Therefore, it seems reasonable to consider that the surface segregation of the lower $M_n$ component is preferable. Also, the entropic effect on the surface enrichment of the lower $M_n$ chains can be understood by taking account of the larger translational entropy of a shorter chain existing at the surface as well as the conformational entropic penalty. The lower $M_n$ chain has a large weight of configuration, $W$, with respect to packing of polymeric chains to unit area compared with the higher one. Since the magnitude of translational entropy is proportional to the natural logarithm of $W$, the shorter chain existing

at the surface has a large translational entropy compared with the longer chain. Thus, it seems reasonable to conclude that the lower $M_n$ component is enriched at the air−polymer interface, even though the lower $M_n$ component has a higher $\gamma_m$. Therefore, the surface segregation of lower $M_n$ PMMA, as shown in Figure 3, is quite reasonable.

## Conclusions

Surface structure and surface molecular motions for the (HMW-PS/LMW-PMMA) blend films were investigated on the basis of XPS and SFM measurements. In the case of the (PS1450k/LMW-PMMA) films of which $M_n$ of PMMA is from 1.2k to 144k, it was revealed from XPS measurement that PMMA was preferentially segregated at the film surface, even though PMMA has higher $\gamma$ compared with that of PS. Surface viscoelastic measurement by SFM revealed that the surface thermal molecular motion of the (PS1450k/PMMA4.2k) film was fairly activated in comparison with the bulk one due to the surface enrichment of LMW-PMMA.

**Acknowledgment.** This work was partially supported by a Grant-in-Aid for Scientific Research on Priority Areas, "New Polymers and Their Nano-Organized Systems" (No.277/08246239), from The Ministry of Education, Science, Sports and Culture of Japan and by Research Fellowships of the Japan Society for the Promotion of Science for Young Scientists.

## References and Notes

(1) Garbassi, F.; Morra, M.; Occhiello, E. *Polymer Surfaces from Physics to Technology*; John Wiley & Sons: Chichester, 1994.
(2) Kajiyama, T.; Tanaka, K.; Ge, S.-R.; Takahara, A. *Prog. Surf. Sci.* **1996**, *52*, 1.
(3) Kumar, S. K.; Russell, T. P. *Macromolecules* **1991**, *24*, 3816.
(4) Krausch, G.; Dai, C.-A.; Kramer, E. J.; Marko, J. F.; Bates, F. S. *Macromolecules* **1993**, *26*, 5566.
(5) Bhatia, Q. S.; Pan, D. H.-K.; Koberstein, J. T. *Macromolecules* **1988**, *21*, 2166.
(6) Tanaka, K.; Yoon, J.-S.; Takahara, A.; Kajiyama, T. *Macromolecules* **1995**, *28*, 934.
(7) Nakanishi, H.; Pincus, P. *J. Chem. Phys.* **1983**, *79*, 997.
(8) Schmidt, I.; Binder, K. *J. Phys. (Paris)* **1985**, *46*, 1631.
(9) Jones, R. A. L.; Kramer, E. J. *Polymer* **1993**, *34*, 115.
(10) (a) Zhao, X.; Zhao, W.; Sokolov, J.; Rafailovich, M. H.; Schwarz, S. A.; Wilkens, B. J.; Jones, R. A. L.; Kramer, E. J. *Macromolecules* **1991**, *24*, 5591. (b) Jones, R. A. L.; Kramer, E. J.; Rafailovich, M. H.; Sokolov, J.; Schwarz, S. A. *Phys. Rev. Lett.* **1989**, *62*, 280.
(11) Mayes, A. M. *Macromolecules* **1994**, *27*, 3114.
(12) (a) Kajiyama, T.; Tanaka, K.; Takahara, A. *Macromolecules* **1995**, *28*, 3482. (b) Tanaka, K.; Takahara, A.; Kajiyama, T. *Acta Polym.* **1995**, *46*, 476.
(13) (a) Tanaka, K.; Taura, A.; Ge, S.-R.; Takahara, A.; Kajiyama, T. *Macromolecules* **1996**, *29*, 3040. (b) Kajiyama, T.; Tanaka, K.; Takahara, A. *Macromolecules* **1997**, *30*, 280.
(14) (a) Affrossman, S.; Hartshorne, M.; Jerome, R.; Pethrick, R. A.; Petitjean, S.; Vilar, M. R. *Macromolecules* **1993**, *26*, 6251. (b) Affrossman, S.; Bertrand, P.; Hartshorne, M.; Kiff, T.; Leonard, D.; Pethrick, R. A.; Richards, R. W. *Macromolecules* **1996**, *29*, 5432.
(15) Sugiyama, K.; Hirao, A.; Nakahama, S. *Macromol. Chem. Phys.* **1996**, *197*, 3149.
(16) (a) Jalbert, C. J.; Koberstein, J. T.; Balaji, R.; Bhatia, Q.; Salvati, L., Jr.; Yilgor, I. *Macromolecules* **1994**, *27*, 2409. (b) Koberstein, J. T. *MRS Bull.* **1996**, *21*, 19.
(17) Elman, J. F.; Johs, B. D.; Long, T. E.; Koberstein, J. T. *Macromolecules* **1994**, *27*, 5341.
(18) Wu, S. *Polymer Interface and Adhesion*; Marcel Dekker: New York, 1982.
(19) Wattenbarger, M. R.; Chan, H. S.; Evans, D. F.; Bloomfield, V. A.; Dill, K. A. *J. Chem. Phys.* **1990**, *93*, 8343.
(20) Wool, R. P. *Polymer Interfaces*; Carl Hanser Verlag: Munchen, 1995.
(21) Hariharan, A.; Kumar, S. K.; Russell, T. P. *Macromolecules* **1990**, *23*, 3584.
(22) Tanaka, K.; Takahara, A.; Kajiyama, T. *Macromolecules* **1996**, *29*, 3232.
(23) Andrade, J. D., Andrade, J. D., Eds. *Surface and Interfacial Aspects of Biomedical Polymers Vol. 1-Surface Chemistry and Physics*; Plenum Press: New York, 1985.
(24) Kajiyama, T.; Tanaka, K.; Ohki, I.; Ge, S.-R.; Yoon, J.-S.; Takahara, A. *Macromolecules* **1994**, *27*, 7932.
(25) Jalbert, C.; Koberstein, J. T.; Yilgor, I.; Gallagher, P.; Krukonis, V. *Macromolecules* **1993**, *26*, 3069.
(26) Owens, D. K.; Wendt, R. C. *J. Appl. Polym. Sci.* **1969**, *13*, 1741.
(27) Kressler, J.; Higashida, N.; Shiomi, K.; Inoue, T.; Ougizawa, T. *Macromolecules* **1994**, *27*, 2448.
(28) Yethiraj, A.; Kumar, S. K.; Hariharan, A.; Schweizer, K. S. *J. Chem. Phys.* **1994**, *100*, 4691.
(29) Ballard, D. G. H.; Wignall, G. D.; Schelten, J. *Eur. Polym. J.* **1973**, *9*, 965.

MA9709866